First Measurement of the 19F(α, p)22Ne Reaction at Energies of Astrophysical Relevance

Pizzone, R.G.; D'Agata, G.; La Cognata, M.; Indelicato, I.; Spitaleri, C.; Blagus, S.; Cherubini, S.; Figuera, P.; Grassi, L.; Guardo, G.L.; ...

Source / Izvornik: **Astrophysical Journal, 2017, 836**

Journal article, Published version
Rad u časopisu, Objavljena verzija rada (izdavačev PDF)

https://doi.org/10.3847/1538-4357/836/1/57

Permanent link / Trajna poveznica: https://urn.nsk.hr/urn:nbn:hr:217:603063

The Astrophysical Journal, 836:57 (6pp), 2017 February 10 https://doi.org/10.3847/1538-4357/836/1/57

First Measurement of the ^{19}F(α, p)^{22}Ne Reaction at Energies of Astrophysical Relevance

R. G. Pizzone[1], G. D'Agata[1,2], M. La Cognata[1], I. Indelicato[1], C. Spitaleri[1,2], S. Blagus[3], S. Cherubini[1,2], P. Figuera[1], L. Grassi[3], G. L. Guardo[1], M. Gulino[1,4], S. Hayakawa[1,5], R. Kshetri[1,6], L. Lamia[1,2], M. Lattuada[1,2], T. Mijatović[3], M. Milin[7], Đ. Miljanić D.[3,8], L. Prepolec[3], G. G. Rapisarda[1], S. Romano[1,2], M. L. Sergi[1], N. Skukan[3], N. Soić[3], V. Tokić[3], A. Tumino[1,4], and M. Uroić[3]
[1] INFN—Laboratori Nazionali del Sud, Catania, Italy; rgpizzone@lns.infn.it
[2] Dipartimento di Fisica e Astronomia, Università degli Studi di Catania, Catania, Italy
[3] Ruđer Bošković Institut, Bijenicka cesta, 54, 10000, Zagreb, HR, Croatia
[4] Facoltà di Ingegneria ed Architettura, Kore University, Viale delle Olimpiadi, 1, I-94100 Enna, Italy
[5] Center for Nuclear Study, the University of Tokyo, RIKEN campus, 2-1 Hirosawa, Wako, 351-0198, Japan
[6] Department of Physics, Sidho-Kanho-Birsha University, Purulia 723104, WB, India
[7] Department of Physics, Faculty of Science, University of Zagreb, Zagreb, Croatia
Received 2016 December 21; revised 2017 January 10; accepted 2017 January 10; published 2017 February 8

Abstract

The observational ^{19}F abundance in stellar environments systematically exceeds the predicted one, thus representing one of the unsolved challenges for stellar modeling. It is therefore clear that further investigation is needed in this field. In this work, we focus our attention on the measurement of the ^{19}F(α, p)^{22}Ne reaction in the astrophysical energy range, between 0.2 and 0.8 MeV (far below the Coulomb barrier, 3.8 MeV), as it represents the main destruction channel in He-rich environments. The lowest energy at which this reaction has been studied with direct measurements is ∼0.66 MeV, covering only the upper tail of the Gamow window, causing the reaction-rate evaluation to be based on extrapolation. To investigate lower energies, the ^{19}F(α, p)^{22}Ne reaction has been studied by means of the Trojan horse method, applied to the quasi-free ^{6}Li(^{19}F, p^{22}Ne)^{2}H reaction at $E_{\rm beam} = 6$ MeV. The indirect cross section of the ^{19}F(α, p)^{22}Ne reaction at energies $\lesssim$1 MeV was extracted, fully covering the astrophysical region of interest and overlapping existing direct data for normalization. Several resonances have been detected for the first time inside the Gamow window. The reaction rate has been calculated, showing an increase up to a factor of 4 with respect to the literature at astrophysical temperatures. This might lead to potential major astrophysical implications.

Key words: nuclear reactions, nucleosynthesis, abundances

1. Astrophysical Motivation

One of the most relevant open issues in astrophysics is the origin of the chemical elements. Although a lot has been done in the last decades to comprehend it, nucleosynthesis is still far from being fully understood. Even among the $A \leqslant 56$ elements, whose production is better understood, there are important cases where the nucleosynthesis of the elements is still uncharted. The only stable isotope of fluorine, ^{19}F, is the least abundant of the elements with $12 \leqslant A \leqslant 32$, and its origin is still a matter of debate. Fluorine is an element of particular interest, as it is extremely sensitive to the physical conditions within stars, so it could be used as a probe of the stellar interior if its nucleosynthesis is well understood (Lugaro et al. 2004).

Three different astrophysical sites are suggested for production of ^{19}F: AGB stars (Jorissen et al. 1992), which are regarded as the major contributors to the Galactic fluorine abundance; type II supernovae (Woosley & Haxton 1988); and Wolf–Rayet stars (Goriely et al. 1989). Nevertheless, the only astrophysical site where it was clearly observed is in AGB stars (Lucatello et al. 2011), where fluorine, once produced in the He intershell region via the ^{18}O(p, α)^{15}N(α, γ)^{19}F reaction chain, can be destroyed by three main reactions. Because of the high abundance of ^{4}He in the intershell region, the ^{19}F(α, p)^{22}Ne is expected to be a dominant depletion link. Another destruction process is the ^{19}F(n, γ)^{20}F reaction, triggered by neutrons produced by the ^{13}C(α, n)^{16}O or the ^{22}Ne(α, n)^{25}Mg reactions. If hydrogen is available in sufficient abundance, fluorine may also be depleted through the very strong ^{19}F(p, α)^{16}O reaction. Such reactions mainly affect fluorine dredged up to the surface and exposed to high temperatures and high p abundance in extra mixing phenomena. Therefore, if the fluorine synthesis mechanism is known, its abundance measured on the stellar surface may allow us to constrain stellar physical parameters and mixing scenarios. However, the observed ^{19}F abundances cannot be explained to date (e.g., Lugaro et al. 2004), and a possible reason is the large uncertainties in the reaction rates involved in fluorine production and destruction.

In particular, the reaction rate for the ^{19}F(α, p)^{22}Ne reaction is affected by a large uncertainty at helium-burning temperatures ($0.4 \leqslant T_9 \leqslant 0.8$) because of the lack of experimental data at astrophysical energies. Even recent nucleosynthesis models (Palacios et al. 2005) rely on the very simplified rate expression of Caughlan & Fowler (1988), based on an optical model approximation for estimating the cross section of compound nuclear reactions with overlapping resonances. This reaction rate is in reasonable agreement with Hauser–Feshbach estimates (Thielemann et al. 1986). In the more recent work of Ugalde et al. (2008), the cross section has been measured, and several previously unobserved resonances have been found in the energy range $E_{c.m.} = 0.66$–1.6 MeV. An R-matrix fit was performed and the reaction rate for astrophysical applications computed. The proposed R-matrix fit accounts for the observed resonances, while extrapolation of the cross section was performed to deduce

[8] Deceased.

the low-energy behavior. Nevertheless, the reduced widths Γ_α of the involved resonances were roughly estimated, and a more precise determination would be necessary. Thus an experimental measurement is needed in the Gamow energy range to better understand fluorine burning in an AGB environment. Because of the strong experimental difficulties arising with the Coulomb barrier, a possible solution, as in other physical cases discussed in the next section, might be given by indirect methods and especially the Trojan horse method (THM).

2. Theoretical Framework

The nuclear reaction cross section for charged particles in a stellar plasma, $\sigma(E_{c.m.})$, is exponentially damped (e.g., nano/picobarn) by the penetration of Coulomb and centrifugal barriers, making it very challenging to precisely measure $\sigma(E_{c.m.})$ at the Gamow energy (E_G) (Rolfs & Kavanagh 1986). This effect, of course, is much more dramatic for α-induced reactions, with respect to reactions triggered by protons, due to the stronger Coulomb suppression. The behavior of the cross section at E_G is usually extrapolated from higher energies where data are available by using the smoother astrophysical factor $S(E_{c.m.})$.

To avoid extrapolation, a number of experimental solutions were proposed to enhance the signal-to-noise ratio at E_G in direct measurements, such as underground laboratories like the LUNA project. Even in those cases where energies of astrophysical interest are attained, measurements in the laboratory suffer from the effect of electron screening (Assenbaum et al. 1987). In order to overcome the difficulties affecting direct measurements, the THM has been introduced, and it has proved to be one of the most powerful tools for investigating charged-particle-induced reactions at sub-Coulomb energies (see Tribble et al. 2014; Spitaleri et al. 2016 for reviews of the method). The THM was discussed for the first time in Baur (1986) and Spitaleri (1991). It has been successfully applied to several fundamental astrophysical problems, such as primordial nucleosynthesis (Rinollo et al. 2005; Pizzone et al. 2014; Tumino et al. 2014; Li et al. 2015), the lithium problem (Pizzone et al. 2005b; Lamia et al. 2012, 2013), light element depletion (Spitaleri et al. 2014; Lamia et al. 2015), AGB stars (La Cognata et al. 2009; Palmerini et al. 2013), and nova nucleosynthesis (Sergi et al. 2015). Recently, the method has proven suitable for measurements involving radioactive ion beams (Cherubini et al. 2015; Pizzone et al. 2016) and neutrons (Gulino et al. 2013), thus proving its wide applicability. The idea of the THM is to extract the cross section of an astrophysically relevant two-body reaction

$$A + x \rightarrow c + C \tag{1}$$

at low energies from a suitably chosen quasi-free (QF) three-body reaction:

$$A + a \rightarrow c + C + s, \tag{2}$$

where particle a has a strong $x \oplus s$ cluster structure. Under QF kinematic conditions, s acts as a spectator to the $A + x$ interaction, and the cross section of the $A + x \rightarrow c + C$ process can be deduced with the help of direct reaction theory. In the present case, we will take advantage of the well-known $^6\mathrm{Li} = \alpha \oplus d$ structure with α acting as a participant and d as a spectator. If the bombarding energy E_A is chosen high enough to overcome the Coulomb barrier in the entrance channel of the $A + a \rightarrow c + C + s$ reaction, the deduced $A + x \rightarrow c + C$ cross section is devoid of Coulomb suppression and, owing to the large energies involved, of electron screening effects. The validity of such a participant spectator mechanism has been extensively verified (Pizzone et al. 2013).

These considerations are supported by a more advanced theoretical treatment (Mukhamedzhanov et al. 2008; La Cognata et al. 2009, 2013, 2015), here discussed in brief. The TH reaction amplitude describing the transfer of particle x is given in the post form by

$$M(P, \boldsymbol{k}_{aA}) = \langle \chi^{(-)}_{\boldsymbol{k}_{sF}} \Phi^{(-)}_F | \Delta V_{sF} | \Psi^{(+)}_i \rangle. \tag{3}$$

Here, $\Psi^{(+)}_i$ is the exact $a + A$ scattering wave function; $\Phi^{(-)}_F$ is the wave function of the system $F = c + C = x + A$;, $\chi^{(-)}_{\boldsymbol{k}_{sF}}(\boldsymbol{r}_{sF})$ is the distorted wave of the system $s + F$; $\boldsymbol{r}_{sF}$ and $\boldsymbol{k}_{sF}$ are the relative coordinate and relative momentum of particles s and F; $P = \{\boldsymbol{k}_{sF}, \mathrm{k}_{cC}\}$ is the six-dimensional momentum describing the three-body system s, c, and C in the final state; $\Delta V_{sF} = V_{sF} - U_{sF}$; $V_{sF} = V_{sc} + V_{sC} = V_{sx} + V_{sA}$ is the interaction potential of s and the system F; and U_{sF} is their optical potential.

Using a shell-model-based R-matrix representation of the $\Phi^{(-)}_{F\,\alpha}$ wave function for channel α, a spectral decomposition is obtained.

This is a key point in the THM theory for resonance reactions, as the same reduced widths and resonance energies appear in the THM half-off energy-shell (HOES) cross section and in the astrophysical factor. Therefore, the fitting of the THM cross section yields the resonance parameters of interest with no need of corrections.

In practical calculations, the exact $M_\tau(\boldsymbol{k}_{sF}, \boldsymbol{k}_{aA})$ can be replaced by the plane wave one. If noninterfering resonances are also considered, triple differential cross section integration over Ω_{cC} is performed, and the dependence on the $x - s$ momentum distribution is removed; thus the THM cross section takes the form (Mukhamedzhanov et al. 2008; La Cognata et al. 2011)

$$\frac{d^2\sigma}{dE_{xA}\,d\Omega_s} = \mathrm{NF} \sum_i (2J_i + 1) \times \left| \sqrt{\frac{k_{cC}}{\mu_{cC}}} \frac{\sqrt{2P_{l_f}(k_{cC}R_{cC})}\, M_i(p_{xA}, R_{xA})\, \gamma^i_{cC}}{D_i(E_{xA})} \right|^2, \tag{4}$$

where NF is a normalization factor, P_{l_f} is the penetration factor in l_f–wave (which is the relative orbital angular momentum of outgoing particles c and C), R_{xA} and R_{cC} are the channel radii, $M_i(p_{xA}, R_{xA})$ is the transfer amplitude for the $a + A \rightarrow F + s$ reaction, and $D_i(E_{xA})$ is the R-matrix denominator (see Mukhamedzhanov 2011 for details).

In Equation (4), it is apparent that the on-energy-shell (OES) and the HOES S factors have the same structure, except for the presence of the Coulomb and centrifugal barrier penetrability in the OES $S(E_{c.m.})$ factor that is missing in the entrance channel of the HOES one. Therefore, by fitting the HOES cross section, which is devoid of electron screening effects but is smeared by energy resolution, the OES one can be obtained, which can be compared with direct data after normalization, since in Plane

Wave Impulse Approximation (PWIA) no absolute units are accessible. Normalization is obtained by scaling the strength of the THM measured resonances to those of direct data in the overlap region.

In this work, we will apply the THM to the QF reaction ^{6}Li (^{19}F, p^{22}Ne)^{2}H in order to retrieve information on the ^{19}F (α, p)^{22}Ne reaction cross section at astrophysical energies.

3. Experimental Setup and Data Analysis

A preliminary indirect measurement of the ^{19}F(α, p)^{22}Ne cross section was performed at Florida State University, using the ^{6}Li(^{19}F, p^{22}Ne)^{2}H reaction, firing a ^{19}F beam at 14 MeV onto a pure ^{6}Li target. A dominant contribution from a state in ^{24}Na (sequential decay mechanism) did not allow us to disentangle the QF contribution and apply the THM formulas to extract the ^{19}F(α, p)^{22}Ne cross section.

The reaction was then studied using the Trojan horse nucleus, ^{6}Li, as projectile and selecting kinematic conditions where the sequential mechanisms were expected to be minimal. The ^{19}F(^{6}Li, p^{22}Ne)^{2}H experiment was performed at the Ruder Bošković Institute (Zagreb, Croatia) using a 6 MeV ^{6}Li beam impinging on a 150 μg cm^{-2} ^{7}LiF target. Following the THM prescriptions, the beam energy was chosen to measure the ^{19}F (α, p)^{22}Ne cross section in the energy region of interest for astrophysics. The detection apparatus was composed of two $\Delta E - E$ telescopes, made with a thin silicon detector (9 μm) and a thick position-sensitive detector (PSD; 500 μm) placed at 12.°3 $\pm$ 7° and 32.°3 $\pm$ 7° for deuterium detection, and with three more PSDs for proton detection (centered at 37.°3, 81°, and 119.°9 on the opposite side with respect to the beam axis, respectively, covering about 10° each). The trigger of the acquisition system was the logic AND between one of the detectors placed at one side of the beam and one on the other side. The angular resolution of each PSD turned out to be around 0.°25 and is crucial for such measurements.

Detectors were calibrated by means of standard α sources, by scattering of protons off the Au target, and by means of the α's arising from the ^{6}Li(^{12}C, α)^{14}N* reaction populating many ^{14}N excited states. Equally spaced grids, placed in front of each PSD, were used for angular calibration.

Outgoing particles were identified by means of the standard $\Delta E - E$ technique. Thus, once we reconstructed the angle of emission and kinetic energy of the undetected particle, under the hypothesis it was ^{22}Ne, the experimental Q value was deduced for the selected events. A distribution peaked at 0.18 was retrieved, in good agreement with the theoretical Q value (0.199 MeV). Additionally, the comparison between the experimental proton–deuteron kinematic locus and the simulated one makes us confident of our good reaction channel selection and detector calibration. The technique described in Costanzo et al. (1990) was applied to determine the mass of the undetected particle and estimate the presence of background reactions having p and d in the exit channel. A background level lower than 5% was found. Eventually, only events belonging to the ^{6}Li(^{19}F, p^{22}Ne)^{2}H channel were used for further analysis.

Then, it was checked whether the reaction proceeds via a QF process. Compelling evidence for the occurrence of such a mechanism is provided by the observed agreement between the experimental momentum distribution of the deuterium inside ^{6}Li and the theoretical one given by the square of the Hänckel wave function in momentum space (Pizzone et al. 2005a). In the $p_s \leqslant 55$ MeV c^{-1} region, a good agreement is found, so only events satisfying such a constraint were considered in the extraction of the QF cross section $d^3\sigma/dE_{c.m.}d\Omega_{c.m.}d\Omega_d$ of the ^{6}Li(^{19}F, p^{22}Ne)^{2}H reaction, since this is a necessary condition for the QF mechanism being present and dominant (Shapiro et al. 1965). It was also verified that the measured full width of the momentum distribution ($\sim$50 MeV c^{-1}) agrees with what is expected on the basis of the Pizzone et al. (2005a) work, predicting the momentum distribution FWHM as a function of the transferred momentum.

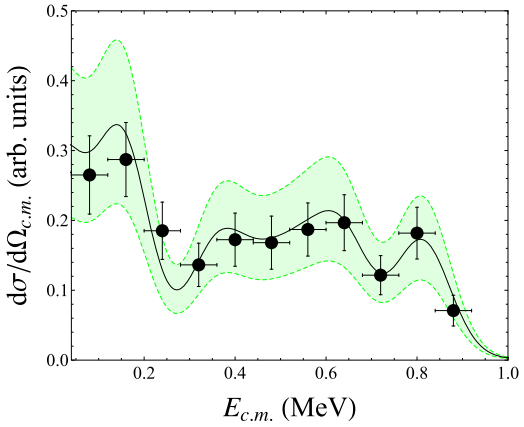

Figure 1. HOES ^{19}F(α, p)^{22}Ne cross section extracted via the THM as a function of $E_{c.m.}$. The experimental cross section (black circles) was fitted using the modified R-matrix formulas. The error bars account only for the statistical errors. The resulting best fit is shown as a solid line, while the band enclosed by the short-dashed lines represents the uncertainty in the R-matrix fit.

4. Results

The HOES cross section for the binary ^{19}F(α, p)^{22}Ne reaction was extracted after dividing the measured $d^3\sigma/dE_{c.m.}d\Omega_{c.m.}d\Omega_d$ cross section by the kinematic factor and by the momentum distribution of the α–d relative motion inside ^{6}Li, as discussed in the previous sections. The experimental HOES cross section as a function of $E_{c.m.} = E_{cC} - Q_{2b}$ (with E_{cC} the relative energy of the ejectiles and Q_{2b} the Q value of the ^{19}F(α, p)^{22}Ne reaction according to the postcollision prescription) is shown in Figure 1 as black solid circles. The experimental data clearly show the presence of several resonances (some of them partially overlapped) corresponding to states in the compound ^{23}Na nucleus. In fact, taking into account beam straggling in the target, the beam spot size (which was minimized to a 1 mm radius), and the straggling into the layers traversed by the emitted particles, the energy resolution of the present measurement was calculated by means of standard error propagation. A FWHM energy uncertainty $\Delta E_{c.m.} \approx$ 60 keV was so determined, which was accounted for in the following data analysis.

Four resonance groups can be recognized, corresponding to ^{23}Na states centered at around 10.6, 10.8, 11, and 11.2 MeV. To understand which ^{23}Na levels contribute to the HOES cross section, angular distributions were deduced and analyzed. The whole yield was divided into three energy intervals, in order to have enough statistics to perform a significant study. The center-of-mass angle of the proton (for the two-body reaction ^{19}F(α, p)^{22}Ne) was calculated using Equation (19) of La Cognata et al. (2015). The resulting angular distributions are shown as solid circles in Figure 2, where statistical errors only are displayed.

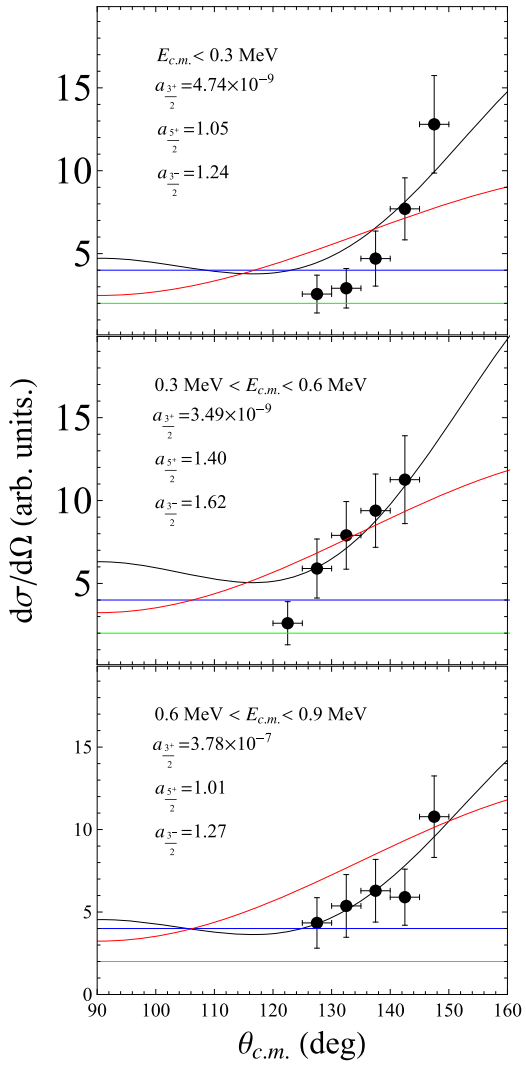

Figure 2. Experimental angular distributions (solid circles) for three center-of-mass energy windows reported in the figure. Here, $\theta_{c.m.}$ is the proton emission angle in the ^{19}F(α, p)^{22}Ne center of mass. The solid black lines represent a fit to the experimental data with a linear combination of $J^\pi = 3/2^+$ and $J^\pi = 5/2^+$ angular distributions calculated using the equations given in Blatt & Biedenharn (1952) and La Cognata et al. (2015). The weights of the two contributions, $a^{3/2^+}$ and $a^{5/2^+}$, are given in the figure. For comparison, the red line represents a fit with the $J^\pi = 3/2^-$ angular distribution (normalization constant being $a^{3/2^-}$) and the green curve a fit with the $J^\pi = 1/2^+$ one (coincident with the angular distribution with $J^\pi = 1/2^-$ (blue line), thus multiplied by 2 to separate them).

The experimental data were fitted by means of a linear combination of $J^\pi = 3/2^+$ and $J^\pi = 5/2^+$ angular distributions, calculated using angular distribution equations for resonant reactions given in Blatt & Biedenharn (1952) and La Cognata et al. (2015). These angular distributions, shown as black lines, agree quite well within the statistical uncertainty with the experimental data, pointing to a dominance of the d wave in the population of resonances lying at $E_{c.m.} \lesssim 0.9$ MeV. Indeed, if angular distributions for p and s waves are computed, a poor comparison with experimental data is retrieved. In detail, p-wave angular distributions are given as red lines in Figure 2 for compound nucleus spin-parity equal to $3/2^-$ and as blue lines for $J^\pi = 1/2^-$. In the case of the s wave, finally, corresponding to a compound spin-parity of $1/2^+$, the angular distributions are marked by a green line. Clearly, these distributions significantly depart from the experimental data. Moreover, the average of the γ_α values measured by Ugalde et al. (2008) are consistent with $l = 2$ predominance in the entrance channel. As a consequence of this study, we proceeded with the analysis of the HOES cross section in the modified R-matrix approach (La Cognata et al. 2011; Spitaleri et al. 2016) to deduce the reduced widths and correct for HOES effects and energy resolution. A weighted fit of the cross section in arbitrary units was performed by means of the modified R-matrix one-level, two-channel formula (La Cognata et al. 2011), assuming $l = 2$ for the entrance channel in the calculations. We used the above approach because of the large error bars affecting the data, making it unnecessary to resort to a more sophisticated calculation that includes interference. Moreover, the energy resolution smears out eventual interference effects. In the calculations, we considered the $l = 2$ levels reported in Table 1 of Keyworth et al. (1968), fixing the resonance energies and the p and p' reduced widths (namely, the ^{23}Na $\rightarrow$ ^{22}Ne + p decays leaving ^{22}Ne in the ground and first excited states, respectively) to those given in Keyworth et al. (1968). The α reduced widths γ_α were fixed to those adopted by Ugalde et al. (2008) above a ^{23}Na excitation energy of $E_R \geqslant 11.15$ MeV and fitted to the THM HOES cross section below. The resonance parameters used in the modified R-matrix calculation are listed in Table 1. The R-matrix fit ($\chi^2 = 0.04$) was performed assuming the proton channel as the dominant one, as pointed out in previous works (Ugalde et al. 2008). This is done also for normalization purposes. The fit was also used to evaluate the resonance contribution to the OES ^{19}F(α, p)^{22}Ne astrophysical factor, according to standard R-matrix formulae. The OES $S(E_{c.m.})$ factor, extracted from the HOES one after taking into account the Coulomb barrier penetration, was determined with the R-matrix parameters reported in Table 1 and is shown in Figure 3 as a black solid line. The green band (representing the total error) arises from the uncertainties in the resonance parameters and from uncertainties in our measurement and takes into account the statistical one as well as the normalization to direct data from Ugalde et al. (2008), the statistical one being the dominant source of errors. The red line represents the available data in the literature (Ugalde

Table 1
Properties of the Investigated Resonances

E_R (MeV)	$E_{c.m.}$ (MeV)	J^π	γ_α (MeV$^{1/2}$)	γ_p (MeV$^{1/2}$)	γ'_p (MeV$^{1/2}$)
10.477	0.01	$3/2^+$	0.001	0.124	0.342
10.616	0.149	$5/2^+$	0.005	0.087	0.327
10.823	0.356	$3/2^+$	0.007	0.131	0.417
10.907	0.44	$5/2^+$	0.001	0.054	0.350
10.972	0.505	$5/2^+$	0.009	0.044	0.184
10.994	0.527	$3/2^+$	0.005	0.011	0.079
11.038	0.571	$3/2^+$	0.003	0.049	0.179
11.109	0.642	$5/2^+$	0.012	0.016	0.096
11.273	0.806	$3/2^+$	0.003*	0.045	0.279
11.280	0.812	$3/2^+$	0.003*	0.127	0.320
11.303	0.836	$3/2^+$	0.003*	0.105	0.148

Notes. Excitation energies, $E_{c.m.}$, J^π, γ_p, and γ'_p taken from Keyworth et al. (1968), while γ_α is fitted to the present experimental data. Values of γ_α marked with an asterisk are taken from Ugalde et al. (2008) and used as fixed parameters for the R-matrix fit.

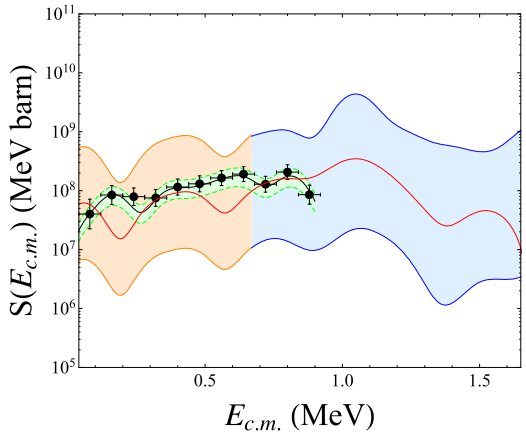

Figure 3. Experimental S factor for the ^{19}F(α, p)^{22}Ne reaction (black circles) as a function of $E_{c.m.}$ fitted with the R-matrix parameterization (solid black line). See text for details.

et al. 2008), smeared to our experimental resolution (using the procedure described in La Cognata et al. 2010).

The blue band represents the total error reported in Ugalde et al. (2008), while the orange band takes into account the average uncertainties in the extrapolation at lower energies performed by Ugalde et al. (2008). Thus, for the first time, the S factor of the ^{19}F(α, p)^{22}Ne reaction is measured in the Gamow energy window, and the contribution of several resonances in the energy range important for astrophysics is outlined.

5. Reaction Rate and Conclusion

The thermonuclear reaction rate at temperature T for ^{19}F(α, p)^{22}Ne is obtained from an average over the Maxwellian velocity distribution:

$$R_{ij} = \frac{N_i N_j}{1+\delta_{ij}}\langle\sigma v\rangle = \frac{N_i N_j}{1+\delta_{ij}}\left(\frac{8}{\pi A}\right)^{\frac{1}{2}}\left(\frac{1}{k_B T}\right)^{\frac{3}{2}} \cdot \int_0^\infty S(E_{c.m.})\exp\left[-\left(\frac{E_{c.m.}}{k_B T} + 2\pi\eta(E_{c.m.})\right)\right]dE_{c.m.} \quad (5)$$

where σ is the fusion cross section, v is the relative velocity of the ij pair, and N_i is the number of nuclei of species i. The result is shown in Figure 4 as a function of temperature. It is evident that for $0.2 < T_9 < 0.5$ the present reaction rate is up to a factor of 4 higher than the one calculated by Ugalde et al. (2008), which is based upon theoretical extrapolations at lower energies. The present result is based on an S factor measured at $E_{c.m.} \leqslant 0.8$ MeV that has shown a series of resonances and might suggest an enhancement in ^{19}F destruction in ^{4}He-rich layers in AGB stars. This updated reaction rate can help us to solve the fluorine puzzle in such stars, giving hints to an enhanced fluorine destruction by means of an (α, p) reaction in the AGB temperature range. For this reason, extensive and more complete calculations are underway to understand the consequences of the present results in astrophysics.

This work was supported by the Italian MIUR under grants no. RBFR082838 and "LNS Astrofisica Nucleare (fondi premiali)."

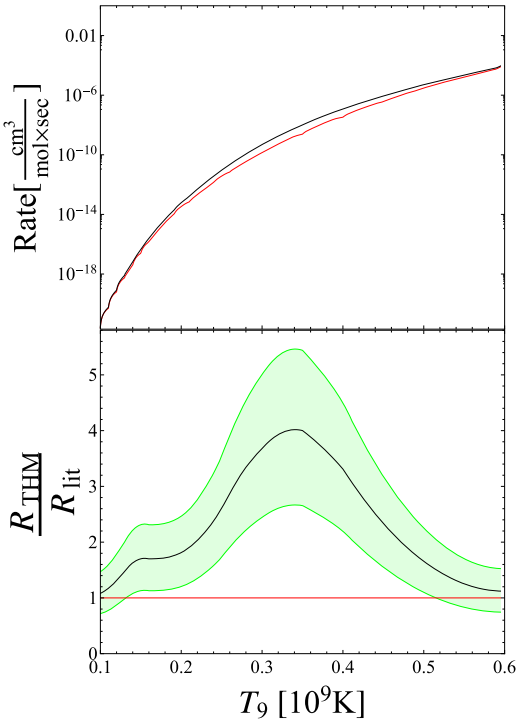

Figure 4. Upper panel: reaction rate for the ^{19}F(α, p)^{22}Ne reactions calculated from the present results (red solid line) compared with those from Ugalde et al. (2008) (black line). Lower panel: ratio of the present reaction rate to the one calculated in Ugalde et al. (2008). The estimated uncertainties of the present data are reported as a green band.

References

Assenbaum, H., Langanke, K., & Rolfs, C. 1987, ZPhyA, 327, 461
Bao, Z. Y., & Kappeler, F. 1987, ADNDT, 36, 411
Baur, G. 1986, PhLB, 178, 135
Blatt, J. M., & Biedenharn, L. C. 1952, RvMP, 24, 258
Caughlan, G. R., & Fowler, W. A. 1988, ADNDT, 40, 283
Cherubini, S., Gulino, M., Spitaleri, C., et al. 2015, PhRvC, 92, 015805
Costanzo, E., Romano, S., et al. 1990, NucIM, 295, 373
Goriely, S. E., Jorrissen, A., & Arnould, M. 1989, in Proc. 5th Workshop on Nuclear Astrophysics, On the mechanisms of 19F production, ed. W. Hillebrandt & E. Muller (Hiedelberg: Astronomisches Rechen-Institut), 60
Gulino, M., Spitaleri, C., Tang, X., et al. 2013, PhRvC, 87, 12801
Jorissen, A., Smith, V. V., & Lambert, D. L. 1992, A&A, 261, 164
Keyworth, G. A., et al. 1968, PhRv, 176
La Cognata, M., Goldberg, V., Mukhamezhanov, A., et al. 2009, PhRvC, 80, 012801
La Cognata, M., Mukhamezhanov, A., Spitaleri, C., et al. 2011, ApJL, 739, L54
La Cognata, M., Palmerini, S., Spitaleri, C., et al. 2015, ApJ, 805, 128
La Cognata, M., Spitaleri, C., Mukhamezhanov, A., et al. 2010, ApJ, 723, 1512
La Cognata, M., Spitaleri, C., Trippella, O., et al. 2013, ApJ, 777, 143
Lamia, L., Spitaleri, C., La Cognata, M., et al. 2012, A&A, 541, 158
Lamia, L., Spitaleri, C., Pizzone, R. G., et al. 2013, ApJ, 768, 65
Lamia, L., Spitaleri, C., Tognelli, E., et al. 2015, ApJ, 811, 99
Lattuada, M., Pizzone, R. G., Typel, S., et al. 2001, ApJ, 562, 1076
Li, C., Wen, Q., Fu, Y., et al. 2015, PhRvC, 92, 025805
Lucatello, S., Masseron, T., Johnson, J. A., Pignatari, M., & Herwig, F. 2011, ApJ, 729, 40
Lugaro, M., Ugalde, C., Karakas, A. I., et al. 2004, ApJ, 615, 934
Mahaux, C., & Weidenmüller, H. A. 1969, Shell-Model Approach to Nuclear Reactions (Amsterdam: North-Holland)
Mukhamedzhanov, A. M. 2011, PhRvC, 84, 044616
Mukhamedzhanov, A. M., Blokhintsev, L. D., Irgaziev, B. F., et al. 2008, JPhG, 35, 014016
Palacios, A., Arnould, M., & Meynet, G. 2005, A&A, 443, 243
Palmerini, S., Sergi, S., La Cognata, M., et al. 2013, ApJ, 764, 128
Pizzone, R. G., Roeder, B., Mckluskey, M., et al. 2016, EPJA, 52, 24

Pizzone, R. G., Spartá, R., Bertulani, C., et al. 2014, ApJ, 786, 112
Pizzone, R. G., Spitaleri, C., Bertulani, C., et al. 2013, PhRvC, 87, 025805
Pizzone, R. G., Spitaleri, C., Cherubini, S., et al. 2005a, PhRvC, 71, 058801
Pizzone, R. G., Tumino, A., Degl'Innoccenti, S., et al. 2005b, A&A, 438, 779
Rinollo, A., Romano, S., Spitaleri, C., et al. 2005, NuPhA, 758, 146c
Rolfs, C., & Kavanagh, R. 1986, NuPhA, 179, 455
Romano, S., Lamia, L., Spitaleri, C., et al. 2006, EPJA, 27, 221
Sergi, M. L., Spitaleri, C., La Cognata, M., et al. 2015, PhRvC, 91, 065803
Shapiro, I. S., Kolybasov, V. M., Augst, G. R., et al. 1965, NucPh, 61, 353
Spitaleri, C. 1991, in Problems of Fundamental Modern Physics II, Proc., ed. R. Cherubini, P. Dalpiaz, & B. Minetti (Singapore: World Scientific), 21
Spitaleri, C., La Cognata, M., Lamia, L., et al. 2016, EPJA, 52, 77
Spitaleri, C., Lamia, L., Puglia, S. M. R., et al. 2014, PhRvC, 90, 035801
Spitaleri, C., Mukhamezhanov, A., Blokhintsev, L., et al. 2011, PAN, 74, 1725
Spitaleri, C., Typel, S., Pizzone, R. G., et al. 2001, PhRvC, 63, 055801
Thielemann, F.-K., Arnould, M., & Truran, J. W. 1986, MPA Rep. No. 262, 15
Tribble, R. E., Bertulani, C., La Cognata, M., et al. 2014, RPPh, 77, 106901
Tumino, A., Spartá, R., Spitaleri, C., et al. 2014, ApJ, 785, 96
Tumino, A., Spitaleri, C., Mukhamezhanov, A., et al. 2008, PhRvC, 78, 064001
Ugalde, C., Azuma, R. E., Couture, A., et al. 2008, PhRvC, 77, 035801
Woosley, S. E., & Haxton, W. C. 1988, Natur, 334, 45